3D bedrock structure of Okayama plain, west Japan, as inferred from gravity anomalies and its relation to damage distribution during the 1946, M8.0, Nankai earthquake

K.Nishimura & J.Akamatsu
Okayama University of Science, Okayama, Japan

M.Komazawa
Geological Survey of Japan, AIST, Tsukuba, Japan

SUMMARY:
Precise gravity measurements, conducted at 7692 stations with spacing of about 300m, revealed 3D structure of granitic bedrock under the Okayama plain, west Japan, which experienced heavy damage during the 1946 Nankai earthquake. Comparison of the obtained bedrock structure with the damage distribution showed that, there was a close spatial correlation between the location of valleys or depressions of the bedrock and that of the heavily damaged zones. Taking this into account, the effect of 3D focusing of seismic waves due to the bedrock topography was examined assuming plane S-waves arriving from the source area of the Nankai earthquake. As a result, it was found that most of damaged houses were distributed near along the valleys where seismic rays focused. This suggests that the effect of bedrock topography on earthquake ground motion should be taken into consideration for seismic hazard assessment.

Keywords: gravity survey, 3D bedrock topography, seismic ray focusing, distribution of earthquake damage

1. INTRODUCTION

Despite being located more than 100km far from the source area, the Okayama plain experienced heavy damage during the 1946, M8.0, Nankai earthquake: according to a document of the local authorities, 52 people lost their lives, 1201 houses were completely destroyed and more than 2300 others were partially destroyed. Since most of damaged houses were distributed in the reclaimed lands of the plain, it has long been believed that the shallow soft soil, characteristic of reclaimed lands, was responsible for the earthquake disaster. It should be noted, however, that the damaged houses were not distributed uniformly, but rather concentrated in some heavily damaged zones. Such non-uniform distribution of damage can hardly be attributed merely to the shallow soil, because near-surface geologic conditions are almost identical throughout the reclaimed lands. This led us to consider the effects of bedrock structure on earthquake ground shaking; especially, focusing of seismic waves due to bedrock topography, which acts like an acoustic lens, is likely to have caused the concentrated distribution of damage, as was the case of the 1994 Northridge earthquake (Gao et al., 1996; Davis et al., 2000) and the 1995 Kobe earthquake (Shiono et al., 1996).

In this study, we investigated 3D bedrock structure under the Okayama Plain by means of gravity survey, and then we examined the effect of 3D focusing of seismic waves by tracing the seismic rays of plane S-waves, arriving from the source area of the 1946 Nankai earthquake. The resultant bedrock structure and focusing effect were compared with the distribution of damage caused by the earthquake.

2. GEOLOGICAL SETTING OF STUDY AREA

The study area, the Okayama plain, is located in the southern part of the Okayama prefecture, west Japan, as shown in Figure.2.1. Major parts of the plain were reclaimed step by step during the period from the 17th century to the middle 20th, but some parts of the plain were reclaimed during the fifties and sixties of the 20th century, and so they did not experience the 1946 Nankai earthquake. Hills and mountains, surrounding or being scattered in the plain, are composed mainly of middle Cretaceous to early Paleogene granitic rocks. Although most of boreholes drilled in the plain are stopped within shallow sediments, there are some boreholes which penetrate into granitic rocks underlying the sediments. Thus, it is highly probable that bedrock under the Okayama plain is composed of granitic rocks.

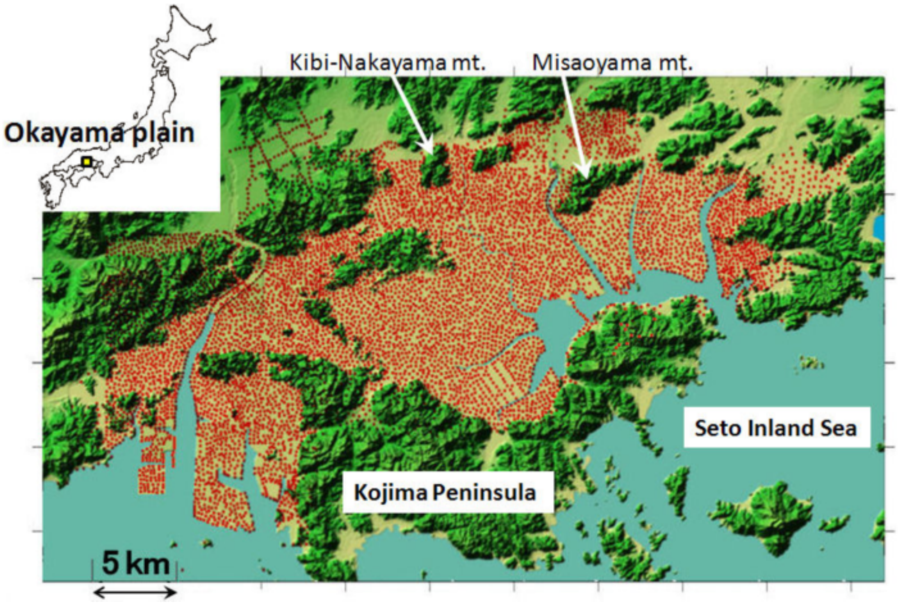

Figure 2.1. Surface topography of Okayama plain and its surroundings, with 7692 gravity stations plotted. Inset at the upper left corner shows the location of the study area in Japan.

3. GRAVITY MEASUREMENTS AND DATA PROCESSING

Gravity measurements were conducted at 7692 stations with spacing of about 300m on the flatland, including urbanized or industrial areas, and 300 to 1000m on the hills and mountains (see Fig. 2.1.), using a portable relative gravimeter CG-3M with quoted accuracy of < 5μGal and reading resolution of 1μGal (Seigel,1995). The location and altitude of the stations were determined by differential GPS (static relative positioning), with use of data from roving receivers placed at gravity stations and those from adjacent reference receivers provided by Geographical Institute of Japan. In order to assess the accuracy of measured data, we carried out repeated or simultaneous measurements at selected 43 stations, using two sets of gravimeter and GPS receiver, and then it was found that, the difference in altitude-corrected absolute value of gravity at one and the same station was less than 50μGal, which was considered to be accurate enough for the present gravity survey.

The bulk density of hills and mountains, needed for terrain and Bouguer corrections, were estimated with the method of gravimetric density determination developed by Parasnis (1952) after Nettleton (1939). As a result, the averaged density of these topographic masses was determined to be 2.60g/cm^3. Terrain corrections were carried out using 50m- and 200m-DEM, respectively, for the distance up to 500m and for that from 500m to 60km around the stations. Bouguer gravity anomalies were computed by taking account of the effect of earth’s curvature, in addition to that of ordinary infinite horizontal plate. Gridding of the gravity anomalies needed for subsequent analysis was carried out with a quadratic regression method to obtain smoothly interpolated data at grid spacing of 100m.

The distribution of the observed Bouguer gravity anomalies is shown as a contour map in Fig. 3.1. As seen from the map, the values of the gravity anomalies are positive all over the study area. This is because the local anomalies reflecting the bedrock topography under the plain are superimposed on long-wavelength regional field which is positive over a wide range including the study area (Murata et al., 2009). Thus, in order to investigate the bedrock structure of interest, the regional gravity field has to be removed from the observed anomalies. This was done by using the upward continuation technique: the gravity field continued upward to 2km, representing long-wavelength components, was subtracted from the observed anomalies to isolate the local components, sometimes called the residual anomalies.

Fig. 3.2 shows the distribution of residual gravity anomalies. It is evident from the figure that values of the anomalies are negative over most of flatland in Okayama plain. This implies that the granitic bedrock under the flatland is overlaid with sediments whose density is less than 2.60g/cm^3.

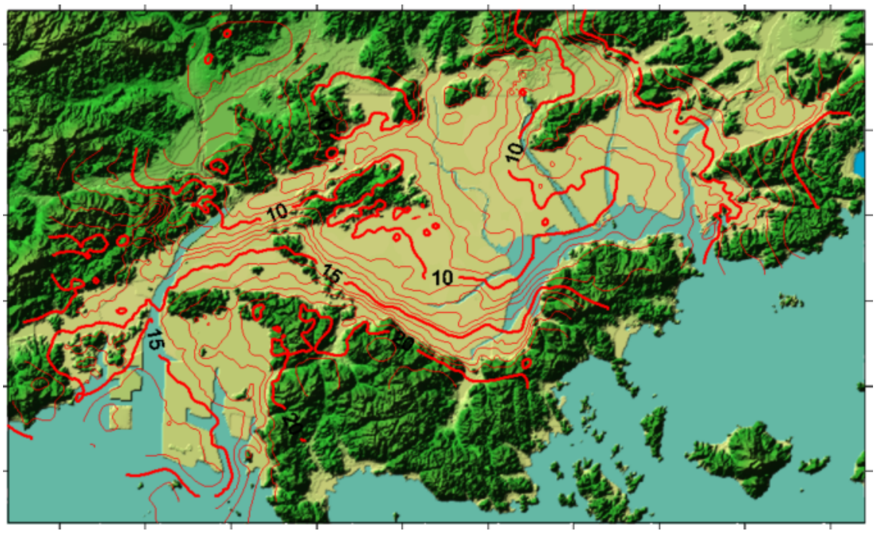

Figure 3.1. Map showing the observed Bouguer anomalies. Assumed density: 2.60g/cm^3. Contour interval: 1mGal. Note that the anomalies are positive all over the study area.

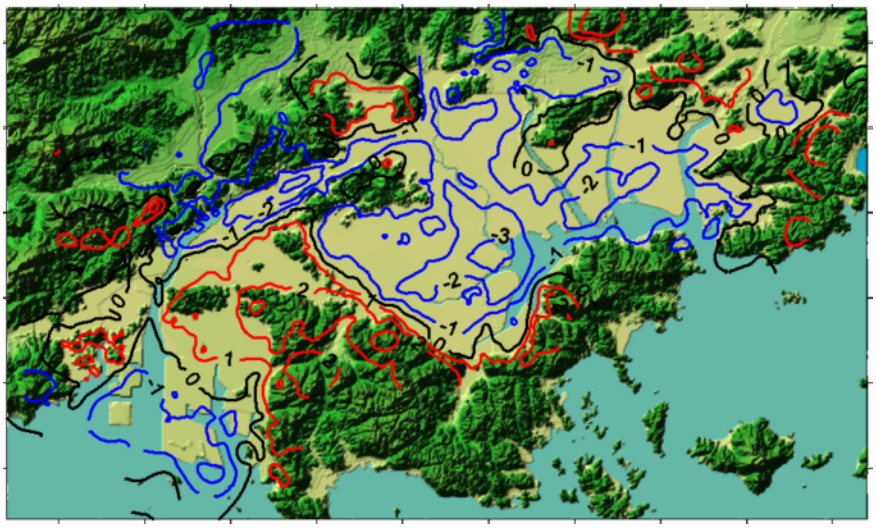

Figure 3.2. Distribution of the residual gravity anomalies, with red, black and blue contour lines indicating positive, zero and negative anomalies, respectively. Contour interval: 1mGal.

4. STRUCTURE OF GRANITIC BEDROCK

The residual gravity anomalies shown in Fig.3.2 were modeled with an inversion method developed by Komazawa (1995) to reveal the 3D bedrock structure. Since information about the internal structure of sediments was insufficient, we assumed a simple structure consisting of a single homogeneous sedimentary layer over the granitic bedrock. Mean density of the sedimentary layer was estimated by 2D modeling of the observed gravity anomalies along six profiles crossing the plain. Thus, in the modeling that follows, the density of granitic bedrock was assumed to be 2.60g/cm^3 and that of sediments represented by a single layer to be 2.20g/cm^3.

As is well known, the interpretation of gravity anomalies is inherently ambiguous, because any given anomaly could be caused by an infinite number of possible sources. In this study, as an external constraint to decrease the ambiguity, we used information about the depth to bedrock derived from boreholes penetrating into the bedrock. For added control on the structural model, we assumed the depth to bedrock to be 30m at the foot of some hills and mountains where no borehole data are available.

Using the densities and the external constraint mentioned above, we determined the depth to bedrock at each grid point through iterative inversion to obtain a 3D model of bedrock structure. The resultant model is shown as a relief map in Fig.4.1 and as a bird's-eye view from east in Fig.4.2. In these figures are shown only those parts of the structural model that are constrained well by gravity data.

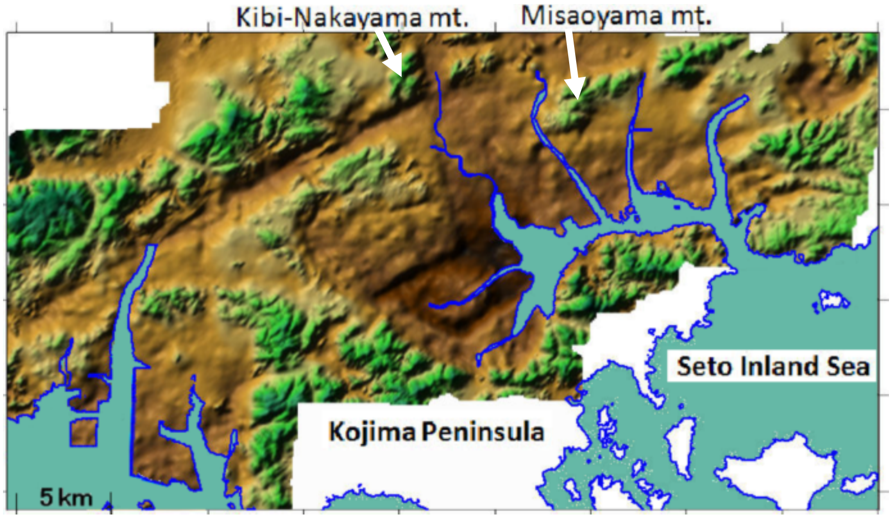

Figure 4.1. Relief map showing 3D bedrock topography.

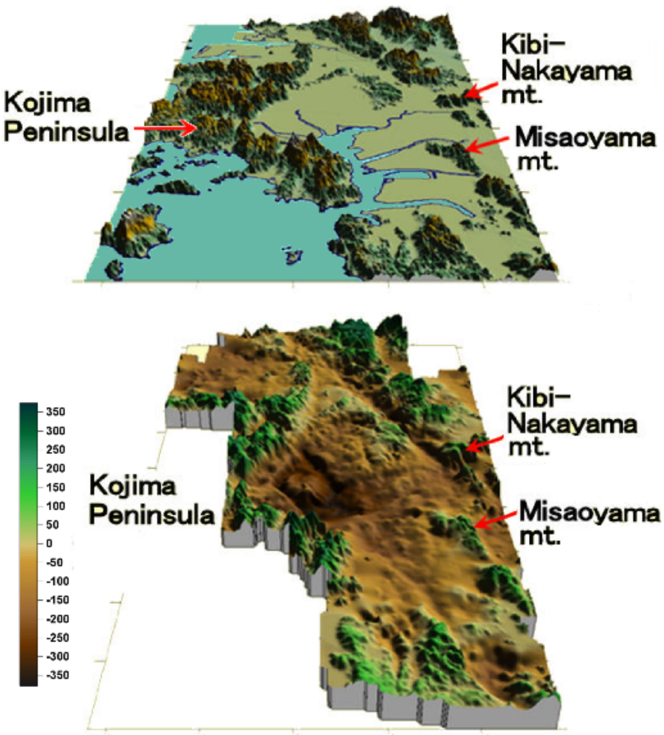

Figure 4.2. Bird's-eye view from east, with upper panel showing surface topography and lower one the bedrock structure.

Main features observed from the bedrock structure, shown in Figs. 4.1 and 4.2, are as follows. There is a deep depression of bedrock in the middle of the Okayama plain, with its maximum depth exceeding 350m. To the southwest of this depression, a small swell of bedrock is found to be encircled by narrow valleys with its maximum depth being about 300m. These valleys seem to be included in an NE-SW-oriented trough crossing the southeastern part of the plain. In the direction perpendicular to this trough, a wide depression extends northwards to the edge of the plain. Another remarkable feature of the bedrock structure is that, there is an NE-SW-oriented valley extending over a length of 30km or more along the northwestern edge of the plain, with its maximum depth exceeding 200m.

5. FOCUSING OF SEISMIC WAVES DUE TO BEDROCK TOPOGRAPHY

Since this study was concerned with the distribution of damage during the 1946 Nankai earthquake, we examined the effect of bedrock topography on the earthquake ground shaking produced by seismic waves arriving from the source area of the earthquake. Assuming that the earthquake damage was caused mainly by S waves, we traced the seismic rays of plane S-waves which focus or defocus at the ground surface after refracting at the bedrock-to-sediment interface.

In calculation, a structure consisting of a single sedimentary layer over the granitic bedrock was assumed, as was done in the modeling of gravity anomalies mentioned above. The 3D bedrock topography was represented by an aggregate of many small planes, each of which was formed by five grid points, one central grid point and four adjacent ones, on the bedrock-to-sediment interface. In this way, dip-angle and dip-direction of the small plane were defined and assigned to the central grid point.

P-wave velocities (Vp), S-wave velocities (Vs) and densities (ρ) of the sedimentary layer and bedrock are shown in Table 5.1. Among them, Vp and Vs were estimated from the distribution of lowest peak frequencies of H/V spectral ratio of microtremors observed at 25 sites in the central part of the study area; at each observation site, the peak frequency was explained by assuming a horizontal sedimentary layer over the bedrock, the thickness of which was already known from the gravity structural model.

Table 5.1. Seismic velocity and density used for calculation

	Vp	Vs	ρ
sediment	1800 m/s	600 m/s	2.20 g/cm^3
bedrock	4600 m/s	2500 m/s	2.60 g/cm^3

Taking the location of source area of the 1946 Nankai earthquake into account, S-wave back-azimuths were assumed to be 120.0° to 215.0° and incident angles measured from the vertical were to be 34.0° to 46.0°, and calculation was conducted at every 2.5 degrees of the back-azimuth and at every 3.0 degrees of the incident angle. The calculated result was expressed as the distribution of the degree of seismic ray concentration at the ground surface as follows; (1) a seismic ray refracted at the central grid point on the small plane, representing a segment of the bedrock-to-sediment interface, was calculated with 3D Snell's law using dip-angle and dip-direction of the plane, and incident angle and back-azimuth of incident wave, (2) a ray tube was formed by the adjacent four rays of incident and refracted waves, and a ratio of area of its horizontal oblique cross-section just below the interface to that at the ground surface was calculated as a measure of the degree of convergence of seismic rays, (3) finally, the ratios of area calculated from seismic rays impinging within 70.7m from each grid point on the ground surface were averaged for all back-azimuths and incident angles of incident waves to obtain the distribution of the degree of seismic ray concentration.

The result of calculation is shown in Fig.5.1, in which the degree of focusing or defocusing of seismic rays is indicated by the color scale; focusing is denoted by warm colors and defocusing by cold colors, and green color indicates that there is no significant focusing nor defocusing. As seen from Fig.5.1, remarkable focusing of seismic rays is confined to the deep and narrow valleys of bedrock, especially along their south to southeast slopes, as expected from the bedrock topography shown in Figs.4.1 and 4.2, and the back-azimuths of incident S waves assumed in the calculation.

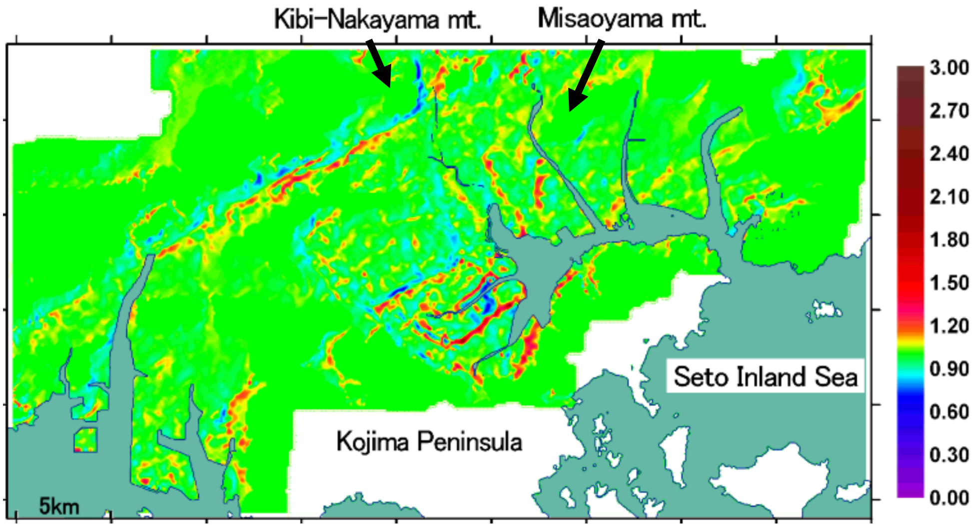

Figure 5.1. Distribution of the degree of focusing or defocusing of seismic rays arriving from the source area of the 1946 Nankai earthquake.

6. COMPARISON WITH THE DISTRIBUTION OF EARTHQUAKE DAMAGE

6.1. Relationship between damage distribution and bedrock topography in the Okayama plain

Information about the distribution of damage in the Okayama plain during the 1946 Nankai earthquake has been provided by several materials, including a reconnaissance report by the local meteorological observatory of Okayama, articles in local newspapers of those days, and chronicles of local history of districts (cities, towns and villages) located in the plain at the time when the earthquake occurred. However, comparison of these materials showed that the number of completely or partially destroyed houses for one and the same district was different from material to material. This was because damage to houses was distinguished from that to barns or granaries in some materials, while in others not distinguished, and because the criteria for judging the extent of damage to house were different among materials. Such being the case, we decided to select a minimum number of completely destroyed houses in each district from among the corresponding numbers given in various materials.

The number of completely destroyed houses in each district thus selected is shown in Fig. 6.1 against a

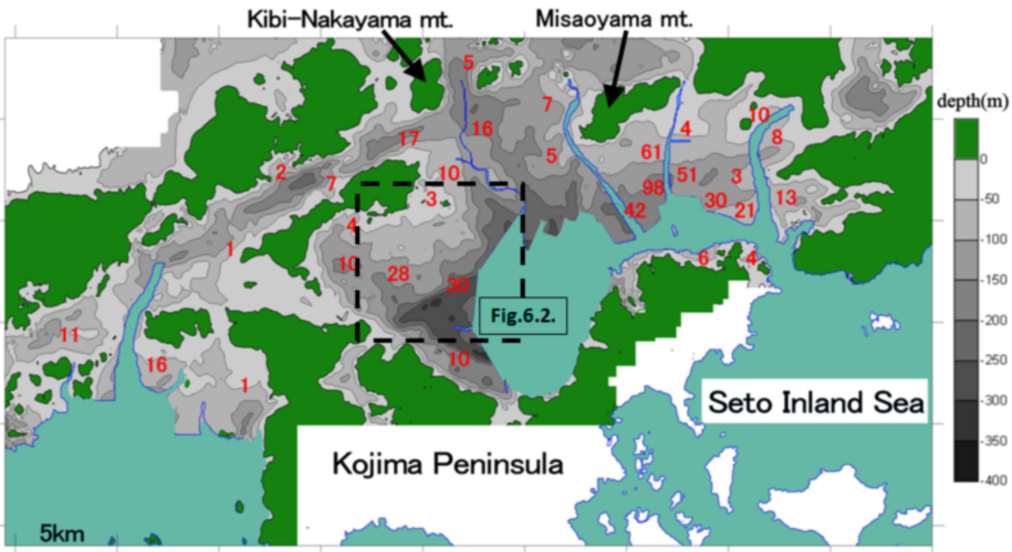

Figure 6.1. Red-colored figures denote the number of completely destroyed houses in each district , shown against a filled contour map of the depth to bedrock. Contour interval=50m.

filled contour map of the depth to bedrock. In this figure, those parts of the Okayama plain reclaimed after the 1946 Nankai earthquake are removed from the map, and the red-colored figures are marked at the center of each district. Although the numbers of completely destroyed houses are not necessarily exact as mentioned above, it is evident from Fig. 6.1 that there is a close spatial correlation between the distribution of heavy damage and the bedrock topography; most of completely destroyed houses were distributed in the areas where the depth to bedrock was relatively large. This suggests that the damage distribution was affected significantly by the bedrock topography.

6.2. Detailed examination of the relationship in a particular area

In order to get more detailed information about the relationship between the damage distribution and the bedrock topography, we examined closely the chronicles of local history of districts, and then we found out some documents which described that, in one and the same district, there had been higher concentrations of damage in some areas than in the immediate surroundings, though the location of individual damaged houses was not provided. As an example of such districts, we took an area enclosed with broken lines in Fig.6.1. The reason why we focused on this area is that the density of houses was almost uniform at the time of the 1946 Nankai earthquake, and that presently available borehole data indicate nearly identical shallow soils throughout the area.

We interviewed 24 elderly people who had experienced the earthquake disaster in their youth to get detailed information about the location of individual damaged houses in the area under consideration. In the interview, most of the people told unanimously that there had been a strong concentration of damage along a belt-like zone in the southern part of the area, and that the boundary between the heavily damaged and the slightly damaged zones had been relatively sharp. As a result of interview, we were able to obtain the exact location of 49 completely destroyed houses, which amounted to about 80% of the total number in the area shown in Fig.6.1.

Fig.6.2 shows the distribution of the completely destroyed houses against a filled contour map of the depth to bedrock (a) and against the map showing degree of focusing or defocusing of seismic rays (b). As seen from the figure, there is a close relationship between the location of the completely destroyed houses, the bedrock topography, and the distribution of the degree of focusing or defocusing of seismic rays. In particular, it is noticeable that the damaged houses were concentrated strongly in the zone situated above the southeast slope of the narrow valley of bedrock (a) and characterized by the high degree of focusing of seismic rays (b). This suggests that the concentrated damage during the 1946 Nankai earthquake was caused by convergence of seismic waves at the ground surface due to the bedrock topography.

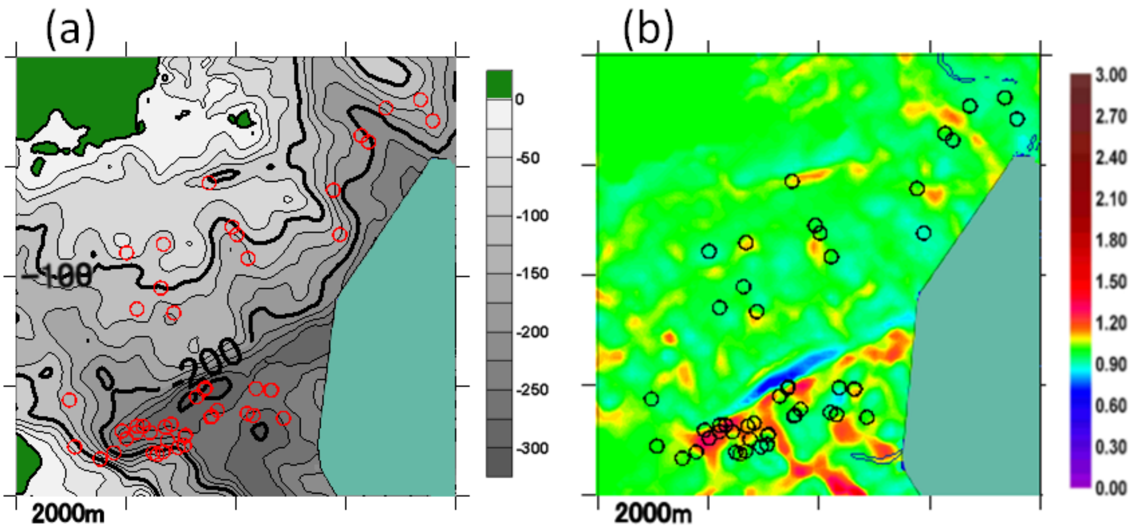

Figure 6.2. Open circles indicate the position of completely destroyed houses in the area enclosed with broken lines in Fig.6.1, plotted (a) against a filled contour map of the depth to bedrock and (b) against the map showing degree of focusing or defocusing of seismic rays.

7. SUMMARY AND CONCLUSION

We conducted precise gravity measurements to reveal 3D structure of granitic bedrock under the Okayama plain, west Japan, which had experienced heavy damage during the 1946 Nankai earthquake. The reason why we focused on the bedrock structure is that there appeared heavily damaged and slightly damaged zones in the plain, despite that its main part has nearly identical shallow soils and was nearly equidistant from the source area of the earthquake.

The obtained structural model exhibited complicated topography of bedrock under the flatland of the plain, and it was found that, in the Okayama plain as a whole, there was a close spatial correlation between the bedrock topography and the distribution of heavy damage; most of completely destroyed houses were distributed in the areas where the depth to bedrock was relatively large.

The effect of bedrock topography on the ground shaking was examined by calculating 3D focusing or defocusing of seismic waves arriving from the source area of the 1946 Nankai earthquake, and then remarkable focusing of seismic rays was found to be confined to the deep and narrow valleys of bedrock, especially along their south to southeast slopes.

In order to make a detailed examination, we selected a particular area where the density of houses was almost uniform at the time of the 1946 Nankai earthquake and near-surface geologic conditions are nearly identical. As a result of examination, a close correlation was found between the location of completely destroyed houses, the bedrock topography and the degree of focusing of seismic waves. This suggests a possibility that the concentrated damage during the Nankai earthquake was caused by convergence of seismic waves at the ground surface due to the bedrock topography.

In this study, we examined the focusing of seismic waves as a possible explanation of the concentrated damage distribution. It is apparent, however, that calculation of ground motion waveforms with use of wave theory is needed for better understanding of the phenomena, because damage to houses is related to the entire history of ground motions.

Although this task is left to future studies, a conclusion derived from the present study is that the effect of bedrock topography on earthquake ground motions should be taken into account for seismic hazard assessment. Besides this, it is worthwhile to point that gravity survey enables us to investigate bedrock structure in detail in urbanized or even industrial areas.

REFERENCES

Davis, P. M., Rubinstein, J. L., Liu, K. H., Gao, S. S. and Knopoff, L. (2000). Northridge earthquake damage caused by geologic focusing of seismic waves, Science, **289**, 1746-1750.

Gao, S., Liu, H., Davis, P.M. and Knopoff, L. (1996). Localized amplification of seismic waves and correlation with damage due to the Northridge earthquake: Evidence for focusing in Santa Monica, Bull. Seis. Soc. Am., **86**, 1B, S209-S230.

Komazawa, M. (1995). Gravimetric analysis of Aso volcano and its interpretation, J. Geod. Soc. Japan, **41**, 17-45.

Murata, Y., Komazawa, M., and 10 others including Nishimura, K. and Akamatsu, J. (2009). Gravity map of Okayama district (Bouguer anomalies), Geological Survey of Japan, AIST.

Nettleton, L.L. (1939). Determination of density for reduction of gravity observations, Geophysics, **4**, 167-183.

Parasnis, D.S. (1952). A study of rock densities in the English Midlands, Mon. Not. R.Astron. Soc., Geophys. Suppl., **6**, 252-271.

Seigel,H. O. (1995). A Guide to High Precision Land Gravimeter Surveys, Scintrex Ltd., Concord, Ontario, Canada.

Shiono, K., Nakagawa, K., Mitamura, M., Masumoto, A. and Irikura, K. (1996). Focusing of seismic waves along the Uemachi fault: Damage in the Osaka area caused by the 1995 Hyogo-ken Nanbu earthquake and a subsurface geologic structure, Jour. of Phys. Earth, **44**, 5, 591-599